Global MHD modeling of the impact of a solar wind pressure change

Kristi A. Keller, Michael Hesse, Maria Kuznetsova, Lutz Rastätter, and Therese Moretto
NASA Goddard Space Flight Center, Greenbelt, Maryland, USA

Tamas I. Gombosi and Darren L. DeZeeuw
Space Physics Research Laboratory, University of Michigan, Ann Arbor, Michigan, USA

Received 26 February 2001; revised 21 December 2001; accepted 21 December 2001; published XX Month 2002.

[1] A sudden increase in the solar wind dynamic pressure compresses the magnetosphere and launches compressional waves into the magnetosphere. The global response of the magnetosphere, including the ionosphere and the location of the field-aligned current (FAC) generation, to a step increase in the solar wind density has been studied using a global three-dimensional adaptive MHD model. As the density increase propagated along the flanks of the magnetopause, a two-phased response was seen in the ionosphere. The first response was an increase in FACs near the polar cap. For this response we found the location of FACs to lie just inside the magnetosphere. The second response was an increase in FACs at lower latitudes. The increase in FACs was in the same direction as region 1 currents. For the second response we found the location of FACs to fall well within the magnetosphere. *INDEX TERMS:* 2784 Magnetospheric Physics: Solar wind/magnetosphere interactions; 2752 Magnetospheric Physics: MHD waves and instabilities; 2753 Magnetospheric Physics: Numerical modeling; *KEYWORDS:* solar wind pressure changes

1. Introduction

[2] The magnetospheric cavity is formed by the interaction of the solar wind with the dipole magnetic field of the Earth. The dynamic pressure of the solar wind greatly compresses the Earth's magnetic field on the dayside, and an extended magnetic tail is formed on the nightside. The dimensions of the magnetosphere depend by and large on the force balance between the streaming solar wind (or the shocked magnetosheath plasma) and the magnetic field of the Earth. On the dayside the radial distance of the magnetopause is thus largely determined by the solar wind ram pressure, i.e., the pressure exerted by the moving plasma density encountering an obstacle.

[3] As a result, changes in solar wind flow velocity or density lead to changes in the magnetopause dimensions. In particular, sudden increases or decreases of solar wind ram pressure can lead to indentations, which propagate along the magnetopause with the ambient magnetosheath flow velocity. Clearly, a propagating disturbance of such a nature will involve a variety of magnetospheric reactions, which have been the subject of a number of recent investigations.

[4] One class of theories about magnetospheric responses to solar wind dynamic pressure changes involves waves along the magnetopause. *Kivelson and Southwood* [1991] and *Sibeck* [1990] proposed that a step-like pressure increase would generate a dual field-aligned current (FAC) system. *Glassmeier and Heppner* [1992] argued that a single pressure gradient would produce a single FAC system while a pressure pulse would generate a dual FAC system. In either case the generation of FACs was considered localized and near the magnetopause.

[5] A second class of theories involves the propagation of compressional waves across field lines through the magnetopause. *Tamao* [1964] suggested that a compression of the magnetosphere could cause a compressional hydromagnetic wave to propagate into the magnetosphere. In the magnetosphere this mode could convert to an Alfvén wave. The Alfvén wave would carry FAC to the ionosphere. *Lysak and Lee* [1992] simulated a pressure pulse hitting the magnetosphere using both single cycle pulses and continuous pulses. In their results, pressure pulses excited compressional waves. These compressional waves could convert to shear mode Alfvén waves due to the inhomogeneity of the Alfvén speed in the magnetosphere. Vortex structures formed on field lines that were resonant with the source frequency. In this case, FAC generation would be inside the magnetosphere.

[6] FACs can be approximated by the following equations [*Ogino*, 1986]:

$$\frac{d\Omega_{\parallel}}{dt} - \frac{\mu}{\rho}\nabla^2\Omega_{\parallel} - \frac{B^2}{\rho}\nabla_{\parallel}\frac{j_{\parallel}}{B} = -\frac{2\mathbf{B}\cdot\nabla p\times\nabla B}{\rho B^2}, \tag{1}$$

$$\frac{\partial j_{\parallel}}{\partial t} - \frac{\eta}{\mu_0}\nabla^2 j_{\parallel} - \frac{1}{\mu_0}\nabla_{\parallel}B\Omega_{\parallel} = 0, \tag{2}$$

where $\Omega_{\parallel}$ is the parallel component of the vorticity, μ is the viscosity, ρ is the density, p is the pressure, $\mathbf{B}$ is the magnetic field, $j_{\parallel}$ is the parallel component of the current density, η is the resistivity, μ_0 is the vacuum magnetic permeability, and $\nabla_{\parallel} = (\mathbf{B}\cdot\nabla)/B$. Equation (1) is similar to those found by *Hasegawa and Sato* [1979]. In both cases it is assumed that $\Omega_{\perp} = 0$. For a uniform pressure the right-hand side (RHS) of equation (1) can be dropped. In that case, *Ogino* [1986] performed a linear analysis of equations (1) and (2) with a perturbation of the form $\exp(\gamma t - \int k_{\parallel}dz)J_0(k_{\perp}r)$, where $J_0(k_{\perp}r)$ is the Bessel function and $k_{\parallel}$ and $k_{\perp}$ are the wave numbers parallel and perpendicular to the magnetic field. For a highly conducting plasma the relationship between $j_{\parallel}$ and $\Omega_{\parallel}$ is

$$j_{\parallel} \approx \frac{-k_{\parallel}B}{|k_{\parallel}B|}\left[\frac{\rho}{\mu_0}\right]^{1/2}\Omega_{\parallel}. \tag{3}$$

[7] In steady state and no viscosity, equation (1) can be integrated along field lines to get [*Vasyliunas*, 1970]

$$\frac{j_{\parallel}}{B} = -\frac{1}{V^{\gamma}}\frac{\mathbf{B}_{eq}}{B_{eq}^2}\cdot[\nabla(pV^{\gamma})\times\nabla V], \tag{4}$$

0148-0227/02/2001JA000060$09.00

where B_{eq} is the magnetic field in the equatorial plane and V is the differential flux tube volume. V is given by

$$V = \int ds/B., \quad (5)$$

where the integration is along closed field lines from the equatorial plane to the ionosphere. The dominant contribution of the integral comes from regions near the equatorial plane where B is smallest. Near the ionosphere, B is significantly larger, and this region makes a smaller contribution to the integral. This discussion shows that there are two possible mechanisms that support FACs. One is based on inertia effects while the other mechanism is pressure based. In this paper, we will investigate which one, if any, is dominant in our simulation.

[8] *Araki* [1994], *Russell and Ginskey* [1995], and *Thorolfsson et al.* [2001] studied ground magnetic signatures of sudden commencements in response to a step-like function increase of the solar wind dynamic pressure increase and found that the waveform of the H component of the ground magnetometer data had two successive pulses with opposite senses. In the morning sector the first pulse is positive and the second pulse is negative. The reverse signature is seen in the afternoon sector. *Araki* [1994] and Thorolfsson et al. (2001) studied southward IMF cases, while *Russell and Ginskey* [1995] considered northward IMF. *Russell and Ginskey* [1995] found that the first pulse lasted about a minute while the second pulse increased for ~5 min then decayed over a 10-min period. Assuming perturbations were consistent with Hall currents flowing low in the ionosphere, *Russell and Ginskey* [1995] concluded that the data was consistent with two sets of vortices and the second set of vortices was moving tailward. For the decrease in pressure, Thorolfsson et al. (2001) found that the signature of the preliminary and main response is opposite to the signature for the pressure increase.

[9] *Moretto et al.* [2000] studied a high-latitude ionospheric response to a sudden impulse event on 23 August 1995. In this event the solar wind IMF increased in magnitude from ~2.5 to ~5 nT. The increase in magnitude was mainly in the B_z component making it even more strongly northward. The northward IMF isolates the response due to sudden commencement from other responses like magnetic reconnection. The density increased from ~2 to 10 cm^{-3} and the solar wind velocity increased from ~310 to ~360 km/s. They used ground magnetic data and a model for the UV conductivity to interpret magnetic data in terms of ionospheric electric potential patterns. The immediate response is a double-cell system in the dayside polar cap that corresponds to FACs flowing into the ionosphere on the duskside and out of the ionosphere on the dawnside. The second response has a double cell of opposite polarity. This system grows in 2 min then slowly decays over 7 min. The system then stabilizes into a steady state system. In contrast with *Russell and Ginskey* [1995], *Moretto et al.* [2000] did not see any tailward movement in the second system.

[10] Pressure pulses have also been simulated by global magnetohydrodynamic (MHD) codes. *Slinker et al.* [1999] simulated a sharp change in density from 5 to 20 cm^{-3} then a linear change back down to 5 cm^{-3} over 5 min. In their simulation the first response is at latitudes centered around 68° magnetic latitude. The ionospheric response has opposing pairs of vortices in both the morning and afternoon sectors. The vortices move tailward on closed field lines and map to a radial distance just outside ≈7 R_E and well away from the magnetopause and low-latitude boundary layer. *Slinker et al.* [1999] concluded that the results were consistent with hydromagnetic waves of *Tamao* [1964] and *Lysak and Lee* [1992]. *Chen et al.* [2000] simulated a tangential discontinuity where the plasma density increases by a factor of 2, temperature decreases by a factor of 2, and the magnetic field remains unchanged. Their results show that twin traveling vortices in the magnetosphere are produced by fast mode waves during early times and later by the transmitted tangential discontinuity. *Chen et al.* [2000, p. 3586] simulation results demonstrate that "Alfvén waves and the associated FACs are generated in the vortices."

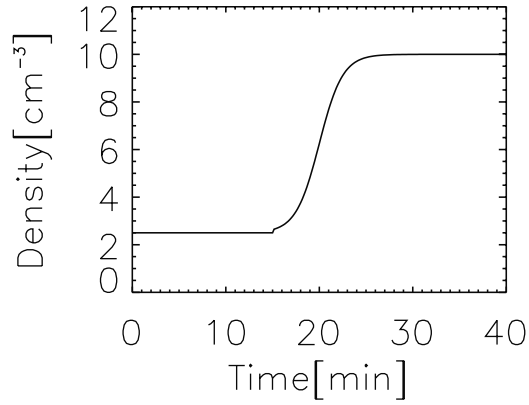

Figure 1. The density input for the solar wind.

[11] In this paper, we present results of a global MHD simulation of a solar wind density increase impacting the magnetosphere when the IMF is northward. An unresolved question left open by *Moretto et al.* [2000] is what drives the second response in the ionosphere during northward IMF periods. In particular, we will look at the source of FACs and the response of the ionosphere. We will compare our results with the above mentioned current theories and observations.

2. Simulation

[12] We used the BATS-R-US code developed at the University of Michigan to solve the MHD equations [*Powell et al.*, 1999]. The simulation code uses an adaptive grid to allow higher resolution in regions of interest. For this simulation the smallest resolution was 0.25 R_E in the inner magnetosphere that extended out from the Earth to ~15 R_E in all three directions. After the startup the grid was fixed for the rest of the simulation run. The number of cells used in the simulation was around 1,900,000. The simulation domain covers −252 to 36 R_E in the GSM x direction, and −48 to 48 R_E in the other two directions. The inner boundary is at 3 R_E. The FACs at 4 R_E are mapped along dipole field lines to the ionosphere (at 110-km altitude) and used to calculate the electrostatic potential. Using FACs at 4 R_E reduces the possible boundary effect on the calculation of FACs. In the ionosphere, constant Pedersen $\sum_p$ = 5 mhos) and vanishing Hall conductivities are chosen for simplicity. The electrostatic potential is mapped back to the magnetosphere to get the velocity and electric field for the boundary.

[13] The solar wind density was increased from 2.5 to 10 cm^{-3} from t = 15 min to t = 25 min (Figure 1) with a very sharp increase from t = 18 min to t = 22 min where the density increased from 3.75 cm^{-3} to 8.75 cm^{-3}. This risetime of four minutes approximates but is slightly longer than the risetime seen in the solar wind data of *Moretto et al.* [2000]. The density profile was rounded off to ensure that the simulation would resolve the jump. The solar wind velocity v_x was kept constant at 340 km/s while v_y and v_z were randomly generated with a maximum of 10 km/s in order to avoid prescription of a specific symmetry. The IMF was constant, oriented northward with a magnitude of 1 nT. The input is similar to the solar wind plasma data from 22 August 1995 [*Moretto et al.*, 2000]. Since our goal was not to model a specific event but to isolate the effect of solar wind density change on the magnetosphere, an average value for v_x and a small northward constant IMF were used.

3. Field-Aligned Current Structure and Location

[14] After the initial setup the simulation was run for 15 min before starting the density increase. This allows the inner magnetosphere to settle down before the density increase impacts the magnetosphere. Overall, the system has not quite reached a steady state, especially in the far tail. The deviation from steady state is small, however, and hence very small current systems are generated in response. The effects of the perturbation by far dominate the current generation by this small deviation from equilibrium.

[15] The leading edge of the solar wind density increase impinges on the magnetopause around t = 22 min. Figure 2a shows the contours of density in the magnetosphere in the equatorial plane before the solar wind density increase. At t = 25 min the density increases at the bow shock and the magnetosheath and, consequently, the magnetosphere starts to compress (Figure 2b). The compression of the magnetosphere moves along the flanks as the solar wind pressure change propagates tailward. This is illustrated in Figure 2c, which shows the increase in density in the magnetosphere on the flanks at t = 35 min. Figure 3 displays the same sequence of events in the noon-midnight plane. Figure 3 demonstrates a strong compression of the dayside magnetosphere,

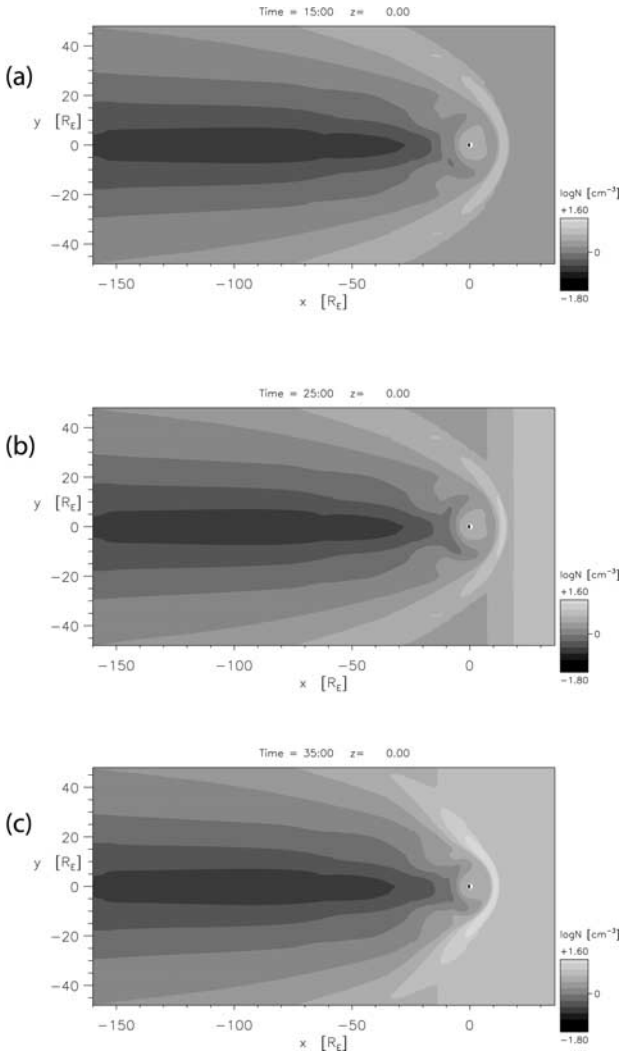

Figure 2. Density contours for (a) t = 15 min, (b) t = 25 min, and (c) t = 35 min for the z = 0 plane. A logarithmic scale is used for the density.

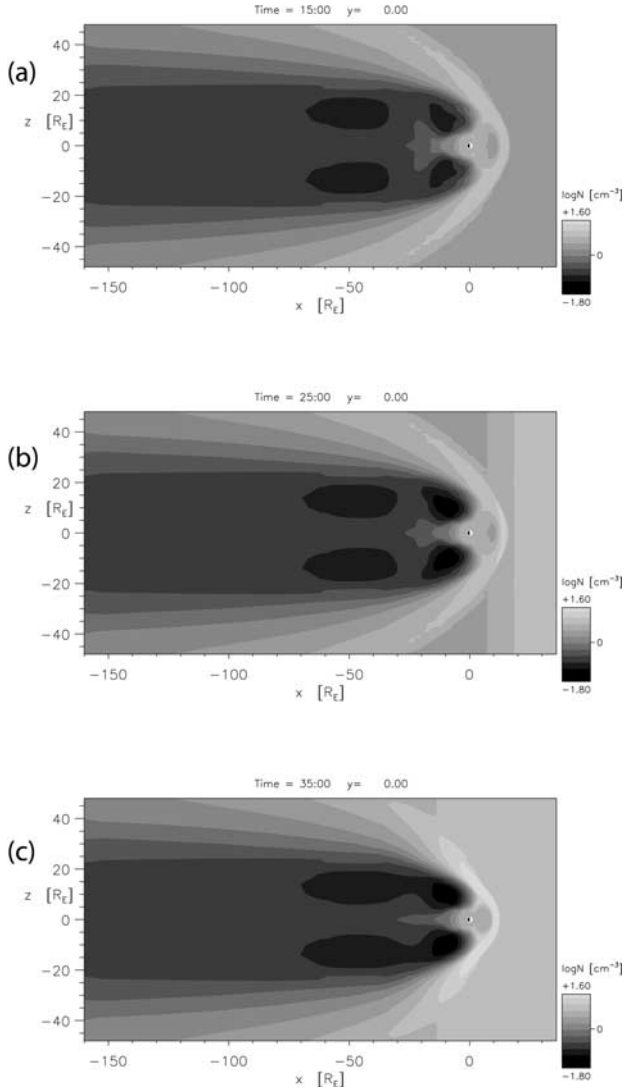

Figure 3. Density contours for (a) t = 15 min, (b) t = 25 min, and (c) t = 35 min for the y = 0 plane. A logarithmic scale is used for the density.

with noticable magnetosheath density intrusions in the cusp regions.

[16] Figure 4a shows the contours of currents into and out of the ionosphere in the northern hemisphere before the impact of the solar wind density increase. Evidently, there is a weak preexisting region 1 current system and an even weaker northward B_z (NBZ) currents, observed during periods of northward IMF northward of the region 1-type current system [*Iijima et al.*, 1984], before the solar wind density increase. The solid line shows the boundary between open and closed field lines. The ionosphere in the Southern Hemisphere is similar. The first signature in the ionosphere of the pressure increase is an increase in the high-latitude current system around t = 27 min. The currents have the same polarity as NBZ currents. Figure 4b shows the difference in current density at t = 27 min and current density at t = 25 min. At t = 28 min, there is an increase in the currents near 1000 and 1400 MLT. The currents have the same polarity as region 1 currents. At t = 32 min the magnitude of these currents continue to increase in the region from 0600 to 1000 MLT and the region from 1400 to1800 MLT and start to increase in the region from 1800 to 2000 MLT and the region from 0400 to 0600 MLT. Figure 4c shows the difference between current density at t =32 min and t = 25 min. The increase in current

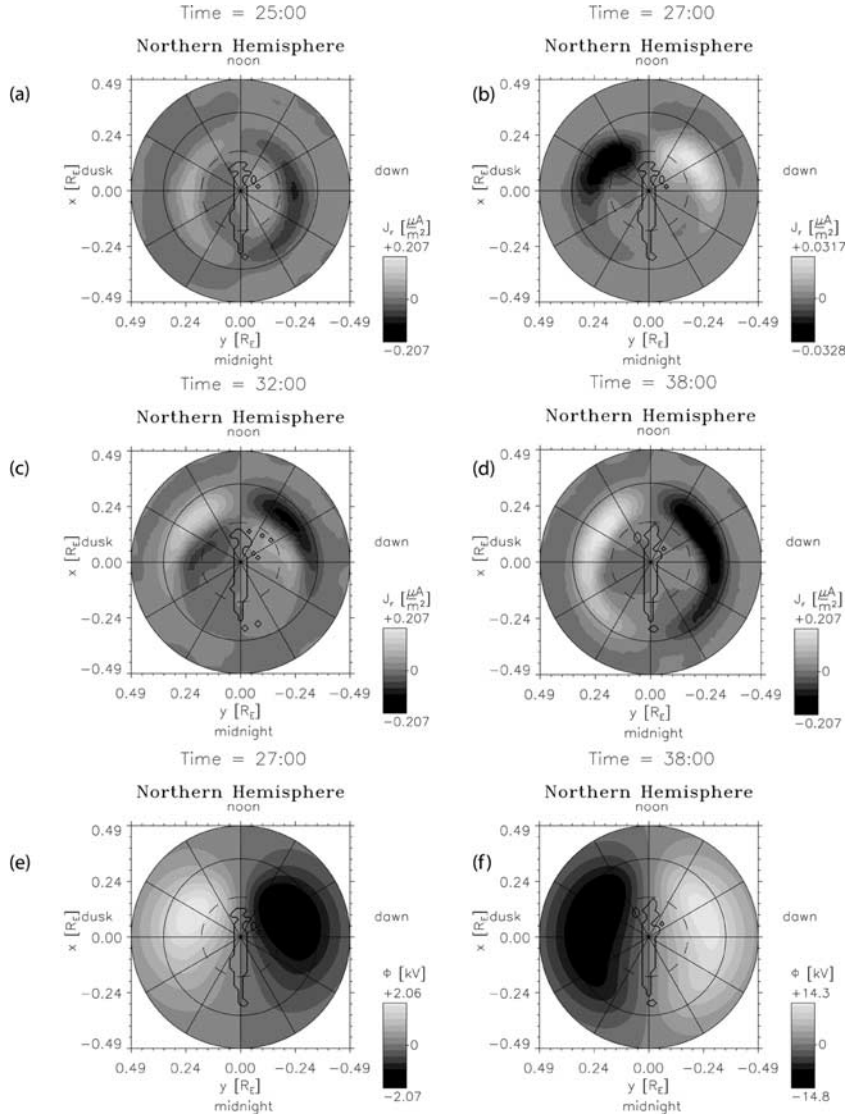

Figure 4. Contours of current density into and out of the ionosphere for (a) $t = 25$ min. Differences in the current density between $t = 25$ min and (b) $t = 27$ min, (c) $t = 32$ min, and (d) $t = 38$ min. Differences in the potential between $t = 25$ min and (e) $t = 27$ min and (f) $t = 38$ min. At $t = 27$ min (Figure 4b) an increase in current density near the polar cap is seen. At $t = 32$ min (Figure 4c) an increase in current density is seen on the dayside of the lower-latitude current system. At later times this increase moves tailward. For current density, positive current is out of the ionosphere and negative current is into the ionosphere. See color version of this figure at back of this issue.

is found deep inside the area of closed field lines. As the pressure increase propagates tailward, the increases in $j_{||}$ move tailward (Figure 4d) also. The largest increase in currents occurs in the regions from 0400 to 1000 MLT and 1400 to 2000 MLT. The currents on the tailward side increase until ~39 min but are always smaller in magnitude than the currents in the regions from 0500 to 1000 MLT and 1400 to 1900 MLT.

[17] The location, sense, and timing of the currents all approximately agree with the results of *Moretto et al.* [2000]. They found that the first response was a double-cell system in the dayside polar cap that corresponded to a set of currents flowing out of the ionosphere on the dawnside and into the ionosphere on the duskside. This system moved slowly poleward and had a 4-min lifetime. *Moretto et al.* [2000] estimated that the shock arrived at the magnetopause around 1306 UT with the first ionospheric signatures occurring at 1307 UT. The first double-cell system lasted to 1311 UT. In our simulation the midpoint of the density increase hits the magnetopause between 26 and 27 min. Small changes in the ionosphere start around $t = 24$ min. The first major signature in the ionosphere is at 27 min in approximate agreement with *Moretto et al.* [2000]. Figure 4e shows the difference in electric potential between $t = 27$ min and $t = 25$ min. This response has the same polarity as the first double cell found by *Moretto et al.* [2000] but has no poleward movement. The electric potential is smaller than the electric potential found by *Moretto et al.* [2000]. The magnitude of the currents increases for ~3 min, and this system has a slightly longer lifetime in the simulation than was seen by *Moretto et al.* [2000]. The second response seen by *Moretto et al.* [2000] was a development of a second double-cell system with opposite polarity at lower latitudes that occurs at 1312 UT ~6 min after the shock. The peaks of both cells are observed moving to higher latitudes as they decay. In the simulation results the second response is an increase in the currents at lower latitudes. These currents have the same polarity as region 1 currents. Figure 4f shows the difference in electric potential between $t = 38$ min and $t = 25$ min. These potential cells have

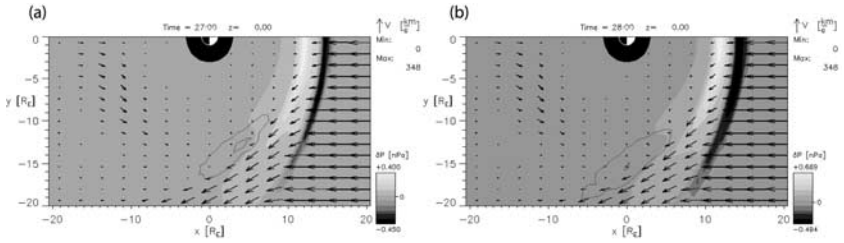

Figure 5. Differences in the pressure between t =25 min and (a) t = 27 min and (b) t = 28 min. The vectors are the velocity at t = 27 min and t = 28 min. The blue contour lines show contours of the newly formed ionospheric current mapped to the equatorial plane along magnetic field lines.

the same polarity and approximate magnitude as the second double-cell system found by *Moretto et al.* [2000] but develop over a longer interval in the simulation and are seen at higher magnetic latitudes due to smaller open flux. In our case we start to see a small increase at 28 min but the larger increase starts 5 min after the midpoint of the density increase hits the magnetopause. The duration of the ionospheric signatures is slightly longer than those found by *Moretto et al.* [2000]. This small difference may be due to the more gradual increase in the density. Besides the difference in the timescale for the density enhancement, there are some other simplifications in the simulation that may contribute to differences between the simulation results and *Moretto et al.* [2000]. First, the simulation uses a simplified constant conductivity model for the ionosphere. Another factor is that there is no dipole tilt used in this simulation. Futhermore, the IMF is constant and smaller than the observed magnetic field. Last, there is no velocity change.

[18] It is important to know the source of the FACs in order to differentiate between the different theories outlined in the introduction. The first response in the ionosphere is a two-cell current pattern forming near the boundary between open and closed field lines as shown in Figures 4b and 4e. The two-cell current pattern has the same polarity as NBZ currents. Figure 5a shows the change in pressure from t = 25 min to t = 27 min along with the velocity vectors at t = 27 min. The newly formed part of the ionospheric current (Figure 4b) occurs on magnetic field lines that map just inside the magnetosphere in the equatorial plane. This area is shown by the blue contours in Figure 5a and is found near the edge of the pressure perturbation. At t = 28 min the pressure perturbations move tailward (Figure 5b). The blue contours show the mapping of the newly formed part of the ionospheric current to the equatorial plane along magnetic field lines and are found near the edge of the pressure perturbation. *Kivelson and Southwood* [1991] proposed that a pressure perturbation would generate Alfvén waves near the magnetopause. The Alfvén waves would generate FACs. The first response is consistent with the theory of *Kivelson and Southwood* [1991].

[19] The second response in the ionosphere is an increase in the currents at lower latitudes. These currents have the same polarity as region 1 currents. This response is significantly larger than the first response. Figure 6a shows the log of positive FACs in a blowup of the near-Earth region at the z = 1 R_E plane for t = 25 min. The region from $x = -12$ R_E to $x = 12$ R_E and from $y = 0$ R_E to $y = 12$ R_E is similar except the FACs are negative. FACs in the $z = 1$ R_E plane start to increase around 28 min. Figure 6b shows the increase in FACs on the dayside at t = 30 min. As the density increase propagates around to the flanks of the magnetopause, the increases in the FACs move tailward (Figure 6c). Figure 6d shows a large increase in the FACs in the region near $x = -9$ R_E, $y = -6$ R_E. The maximum magnitude of the FACs occurs on the nightside around t = 41 min.

[20] While the regions where the FACs are increasing in the magnetosphere move a significant distance in the magnetosphere, the regions of increasing magnitude in the ionosphere move a smaller distance. This is due to the mapping of the magnetic field lines from the magnetosphere to the ionosphere. For a given flux tube cross section in the equatorial plane of the magnetosphere, the flux tube on the dayside maps to a larger region in the ionosphere than a flux tube on the nightside. So as the increases in FACs move tailward in the magnetosphere, the increases in FACs in the ionosphere also move tailward but at a slower rate. Through examination of other z = const planes we can verify that the FACs from these sources flow into the

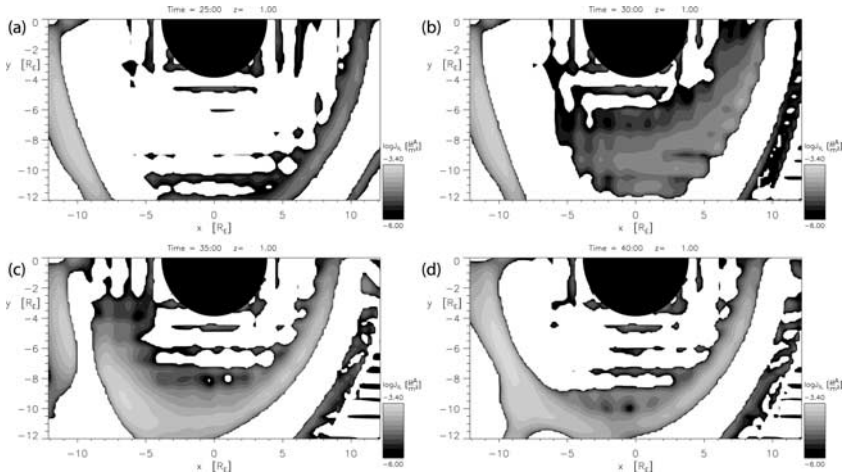

Figure 6. Contours of $j_{||}$ in the $z = 1$ R_E plane for (a) t = 25 min, (b) t = 30 min, (c) t = 35 min, and (d) t = 40 min. An increase in $j_{||}$ starts on the sunward edge at t = 30 min (Figure 6b) then moves tailward with a large increase in $j_{||}$ on the nightside at t = 40 min (Figure 6d). See color version of this figure at back of this issue.

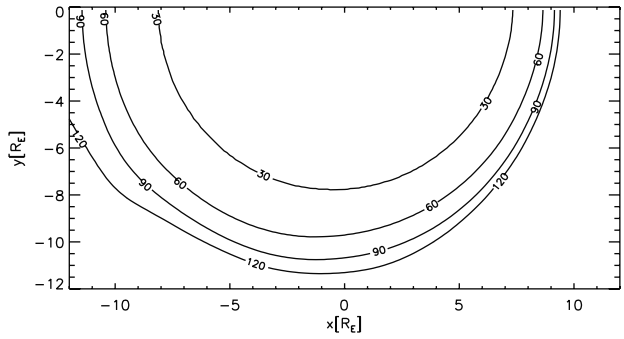

Figure 7. Contours of the Alfvén transit time from the $z = 0$ plane to the ionosphere. Contours are shown for $t = 35$ min in the $z = 0$ plane. The contour levels are 30, 60, 90, and 120 s.

ionosphere. Equation (4) shows that in the absence of sources and inertial effects $j_{||}/B$ is conserved along field lines. Investigating this conservation, we find that $j_{||}/B$ is conserved along field lines within a factor of 2 above $z = 2\ R_E$. Deviations from conservation are caused by one of two effects. One, there is significant divergence of $j_\perp$ to $j_{||}$ below $z = 2\ R_E$ particularly on the nightside. Second, owing to finite Alfvén transit times along the field lines (discussed in more detail in Section 4), we expect that inertial effects limit the validity of equation (4). There is some off-equator closure by current flow perpendicular to the magnetic field for the FACs. A current maxima exists on the nightside at $t = 25$ min before the impact of the pressure pulse. There is closure due to perpendicular current flow so that only part of this current flows into the ionosphere and contributes to part of the preexisting region 1 current system. There is an increase in this current density after the impact of the pressure pulse around $t = 35$ min. While there is an increase in current density in the ionosphere on the tailward side, it does not match the increase on the dayside. This seems to be due to the closure by perpendicular current flow.

[21] The source region of the enhancement in the lower-latitude currents is inside the magnetosphere but, initially, close to the magnetopause on the sunward side. As the current enhancements move tailward, these FACs are found well inside the magnetopause. The FACs in the $z = 1\ R_E$ plane move with the solar wind density increase. As the density increase moves along the magnetopause, the density perturbations start at the magnetopause and move into the inner part of the magnetosphere. The large increase in FACs is located near these density perturbations. In particular, the FACs on the nightside are collocated with a large density perturbation. The perturbation starts on the flank around 30 min into the simulation. The density perturbation does not generate the FACs but is an indicator of the compressional part of the solar wind pressure perturbation.

4. Field-Aligned Currents for the Second Response

[22] The apparent source location of the currents for the second response does not lie at or near the magnetopause. This implies that theoretical models, which predict FAC generation near the magnetopause, for example, through the effects of wave propagation along the magnetopause, do not apply here. Thus the source location of the FACs suggests either FAC generation by mode conversion or by changes in pressure. We found that the computed value of $j_{||}/B$ using equation (4) does not correspond to the values in the ionosphere. This is due to the fact that the Alfvén transit time from the equatorial plane to the ionosphere is comparable to the transit time of the density step increase through the magnetosheath. Figure 7 shows the contours of Alfvén transit time from the equatorial plane to the ionosphere for contour levels of 30, 60, 90, and 120 s. In 120 s the step increase in density propagates $\sim 6\ R_E$. So the step increase propagates through the region of interest before there is enough time for a steady state ($\nabla p \approx \mathbf{J} \times \mathbf{B}$) to be reached along the field lines of interest. The difference in the ionospheric current between $t = 28$ min and $t = 25$ min maps to the dayside near $x = 8\ R_E$ and $y = \pm 4\ R_E$. This corresponds to field lines with an Alfvén transit time from the equatorial plane to the ionosphere between 30 and 60 s. At $t = 30$ min the mapping of the difference in ionospheric current moves toward the flanks and is found on field lines with an Alfvén transit time between 30 and 90 s. At $t = 35$ min the difference in ionospheric current in the ionosphere maps to the dawn and dusk flanks and is found on field lines with an Alfvén transit time between 60 and 150 s.

[23] For further analysis a comparison of the RHS of equation (4) to $j_{||}/B$ at $t = 30$ min shows that the RHS of equation (4) underestimates $j_{||}/B$ on the dayside region especially near $x = 7\ R_E$ and $y = \pm 8\ R_E$. Figure 8 shows the contours of the difference between the RHS of equation (4) and $j_{||}/B$. On the flanks near the region of $x = -3\ R_E$ and $y = \pm 6\ R_E$, the RHS of equation (4) approximates $j_{||}/B$. We also found that equation (3) did not fully account for the magnitude of the FACs in our simulation showing that both the pressure and vorticity terms are significant in this problem. The pressure term in equation (1) is largest at the leading edge of the solar wind density perturbation while the vorticity terms are more significant behind the leading edge of the perturbation.

[24] The changes in pressure are an indicator of the fast mode wave. This fast mode wave mode converts to a shear Alfvén wave. Shear Alfvén waves carry FACs into the ionosphere. The location and timing of the currents in the ionosphere depends on the propagation time of the Alfvén wave along the field line. This is

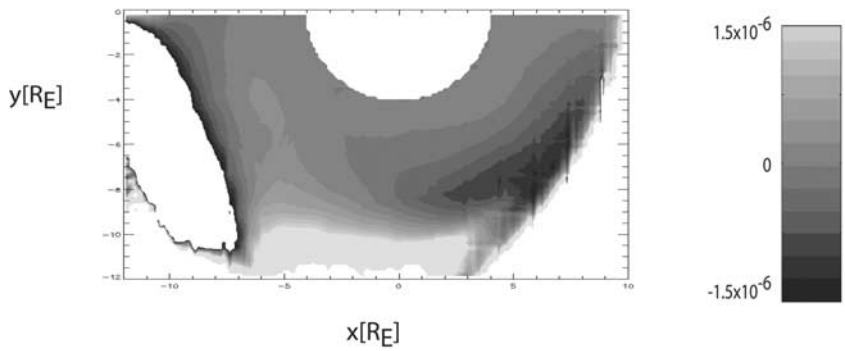

Figure 8. Contours of $[-1/V^\gamma(\mathbf{B}_{eq}/B_{eq}^2) \cdot [\nabla(pV^\gamma) \times \nabla V] - (j_{||}/B)$ for $t = 30$ min. The units are in $\mu A/(m^2\ nT)$. See color version of this figure at back of this issue.

similar to the picture of the Alfvén wing presented by *Glassmeier and Heppner* [1992].

5. Summary

[25] In this simulation a solar wind density increase impacted the magnetosphere around 25 min. This caused an increase in the FACs in the magnetosphere and ionosphere starting around 27 min. The first response in the ionosphere was an increase in the currents at high latitudes at 27 min. The first response was significantly smaller than the second response and was caused by FAC generation just inside the magnetosphere possibly by the mechanism proposed by *Kivelson and Southwood* [1991]. The second and larger response was an increase in the lower latitude currents at 28 min near the sunward edge. As the pressure increase moved antisunward, the increases in FACs moved to the nightside in both the ionosphere and magnetosphere. We investigated in detail the location of FACs for the second response. During the present calculation this location fell well within the magnetosphere, that is, well separated from the magnetopause location. We concluded that FAC generation mechanisms at or near the magnetopause appear not to play a dominant role in the present calculation for the second response. Among all candidate FAC generation mechanisms, this left only two. The first relies on conversion processes between compressional waves directly driven by magnetopause indentations and shear Alfvén waves. The second assumes the dominance of the diamagnetic over the inertial term in the plasma momentum equation. Under this assumption, FACs can be calculated from the divergence of perpendicular, pressure driven, currents. Of these, we investigated in detail the latter, and found that equation (4) is not valid in describing FACs. For the second response our results found that conversion processes between compressional waves directly driven by magnetopause indentations, and shear Alfvén waves were the best candidate for field-aligned current generation. These results were obtained for a relatively slow step increase in the solar wind density. Investigation of field-aligned current generation for a more abrupt solar wind density pulse is the subject of future work.

[26] **Acknowledgments.** This work has benefited from discussions with Aaron Ridley, Gabor Tóth, Kristine Sigsbee, and Paula Reitan. The computational work was done at the Community Coordinated Modeling Center, a multiagency partnership that supports and performs the research and development for next generation space science and space weather models. This work was performed while two of the authors (K.A.K. and T.M.) held a National Research Council Associateship Award at Goddard Space Flight Center. The authors are grateful to the two referees for their comments that have contributed to improving this paper.

[27] Janet G. Luhmann thanks the referees for their assistance in evaluating this paper.

References

Araki, T., A physical model of the geomagnetic sudden commencement, in *Solar Wind Sources of Magnetospheric Ultra-Low-Frequency Waves*, edited by M. J. Engebretson, K. Takahashi, and M. Scholer, *Geophys. Monogr. Ser.*, vol. 81, pp. 183–200, AGU, Washington, D. C., 1994.

Chen, G. X., Y. Lin, and S. Cable, Generation of traveling convection vortices and field-aligned currents in the magnetosphere by response to an interplanetary tangential discontinuity, *Geophys. Res. Lett.*, *27*, 3583, 2000.

Glassmeier, K.-H., and C. Heppner, Traveling magnetospheric convection twin-vortices: Another case study, global characteristics, and a model., *J. Geophys. Res.*, *97*, 3977, 1992.

Hasegawa, A. and T. Sato, Generation of field-aligned currents during substorm, in *Dynamics of the Magnetosphere*, edited by S.-I Akasofu, 529 pp., D. Reidel, Norwell, Mass, 1979.

Iijima, T., T. A. Potemra, L. J. Zanetti, and P. F. Bythrow, Large-scale Birkeland currents in the dayside polar region during strongly northward IMF: A new Birkeland current system, *J. Geophys. Res.*, *89*, 7441, 1984.

Kivelson, M., and D. Southwood, Ionospheric traveling vortex generation by solar wind buffeting of the magnetosphere, *J. Geophys. Res.*, *96*, 1661, 1991.

Lysak, R. L., and D.-H. Lee, Response of the dipole magnetosphere to pressure pulses, *Geophys. Res. Lett.*, *19*, 937, 1992.

Moretto, T., A. J. Ridley, M. J. Engebretson, and O. Rasmussen, High-latitude ionospheric response to a sudden impulse event during northward IMF conditions, *J. Geophys. Res.*, *105*, 2521, 2000.

Ogino, T., A three-dimensional MHD simulation of the interaction of the solar wind with the Earth's magnetosphere: The generation of field-aligned currents, *J. Geophys. Res.*, *91*, 6791, 1986.

Powell, K. G., P. L. Roe, T. J. Linde, T. I. Gombosi, and D. L. De Zeeuw, A solution-adaptive upwind scheme for ideal magnetohydrodynamics, *J. Comput. Phys.*, *154*(2), 284–309, 1999.

Russell, C. T., and M. Ginskey, Sudden impulses at subauroral latitudes: Response for northward interplanetary magnetic field, *J. Geophys. Res., 100*, *23*, 695, 1995.

Sibeck, D. G., A model for the transient magnetospheric response to sudden solar wind dynamic pressure variations, *J. Geophys. Res.*, *95*, 3755, 1990.

Slinker, S. P., J. A. Fedder, W. J. Hughes, and J. G. Lyon, Response of the ionosphere to a density pulse in the solar wind: Simulation of traveling convection vortices, *Geophys. Res. Lett.*, *26*, 3549, 1999.

Tamao, T., A hydromagnetic interpretation of geomagnetic SSC*, *Rep. Ionos. Space Res. Jpn.*, *18*, 16, 1964.

Thorolfsson, A., J.-C. Cerisier, and M. Pinnock, Flow transients in the postnoon ionosphere: The role of solar wind dynamic pressure, *J. Geophys. Res.*, *106*, 1887, 2001.

Vasyliunas, V. M., Mathematical models of magnetospheric convection and its coupling to the ionosphere, in *Particles and Fields in the Magnetosphere*, edited by B. M. McCormac, pp. 60–71, D. Reidel, Norwell, Mass., 1970.

D. L. DeZeeuw and T. I. Gombosi, Space Physics Research Laboratory, University of Michigan, 2455 Hayward, Ann Arbor, MI 48109, USA.

M. Hesse, K. A. Keller, M. Kuznetsova, T. Moretto, and L. Rastätter, NASA Goddard Space Flight Center, Code 696, Greenbelt, MD 20771, USA. (kakeller@pop600.gsfc.nasa.gov)

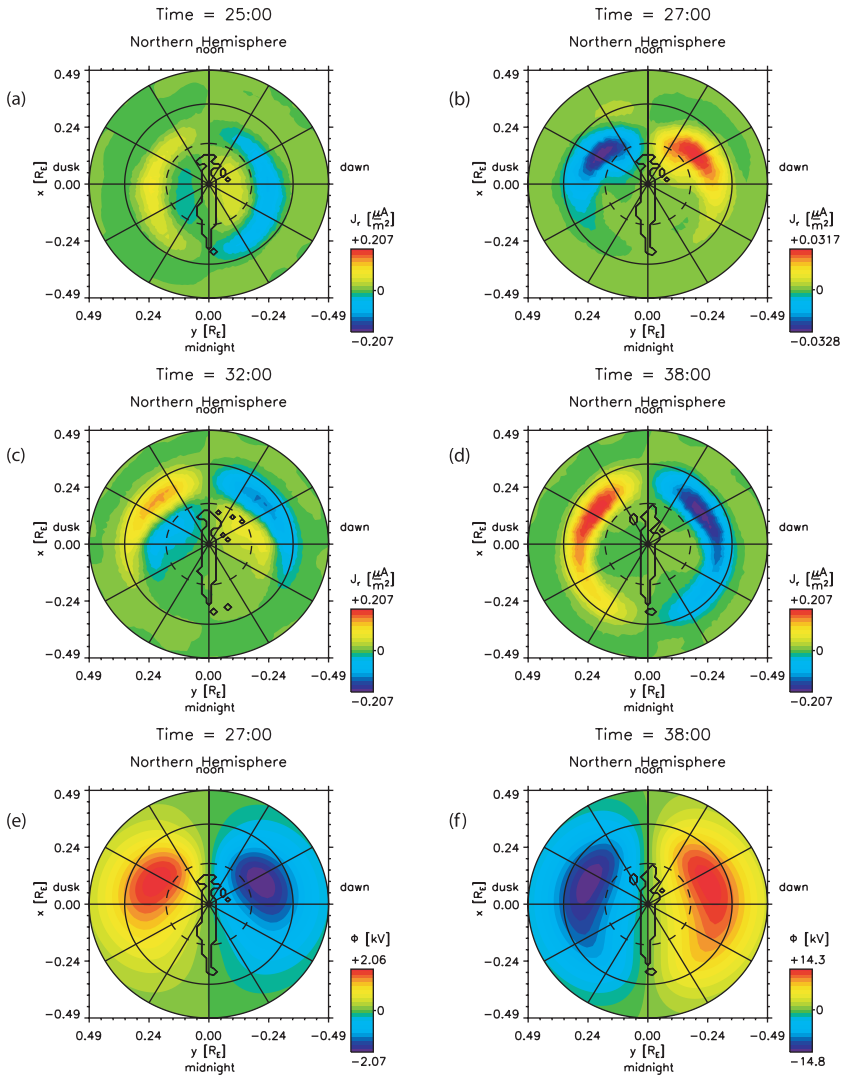

Figure 4. Contours of current density into and out of the ionosphere for (a) $t = 25$ min. Differences in the current density between $t = 25$ min and (b) $t = 27$ min, (c) $t = 32$ min, and (d) $t = 38$ min. Differences in the potential between $t = 25$ min and (e) $t = 27$ min and (f) $t = 38$ min. At $t = 27$ min (Figure 4b) an increase in current density near the polar cap is seen. At $t = 32$ min (Figure 4c) an increase in current density is seen on the dayside of the lower-latitude current system. At later times this increase moves tailward. For current density, positive current is out of the ionosphere and negative current is into the ionosphere.

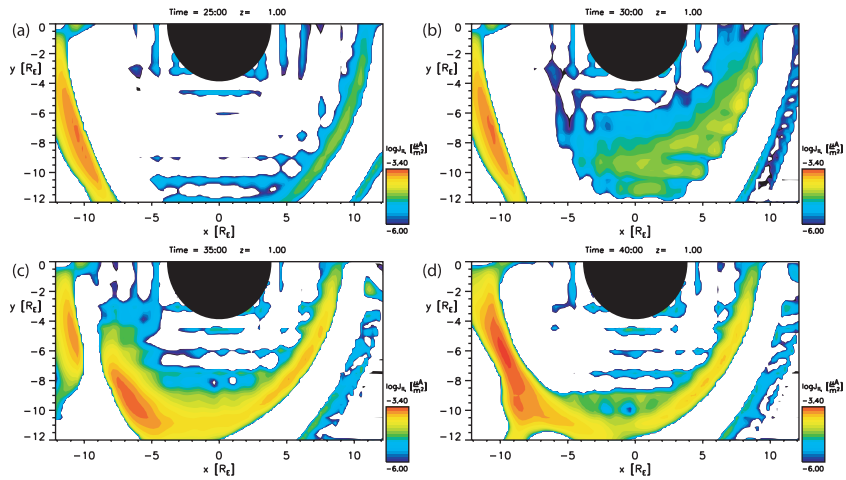

Figure 6. Contours of $j_{||}$ in the $z = 1\ R_E$ plane for (a) $t = 25$ min, (b) $t = 30$ min, (c) $t = 35$ min, and (d) $t = 40$ min. An increase in $j_{||}$ starts on the sunward edge at $t = 30$ min (Figure 6b) then moves tailward with a large increase in $j_{||}$ on the nightside at $t = 40$ min (Figure 6d).

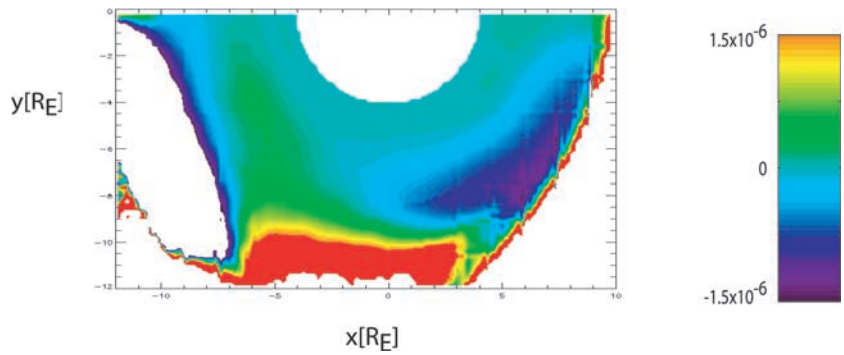

Figure 8. Contours of $\left[-1/V^{\gamma}\left(\mathbf{B}_{eq}/B_{eq}^{2}\right)\cdot\left[\nabla(pV^{\gamma})\times\nabla V\right]-\left(j_{||}/B\right)\right.$ for $t = 30$ min. The units are in μA/(m^2 nT).